Proceedings of the 17th World Congress
The International Federation of Automatic Control
Seoul, Korea, July 6-11, 2008

POWER REDUCTION BY CONTROLLING JOINT COMPLIANCE FOR THE PROPULSION OF A BIOMIMETIC UNDERWATER VEHICLE

Jenhwa Guo and Wei-Kuo Yen

Department of Engineering Science and Ocean Engineering
National Taiwan University
73 Chou-Shan Road, Taipei, Taiwan

Abstract: The work describes a compliance control scheme for the caudal joint motion of a biomimetic autonomous underwater vehicle (BAUV). The purpose of the control method is to use the motor power more effectively for propulsion. A symmetric foil executing large-amplitude sway and yaw motions in a flow imitates a flapping tail fin which is used as the propulsive device of BAUV. Motions of the oscillating foil are then actuated by motors through springs. A control method was derived for the determination of the spring compliance for better use of the motors' driving power. It is verified that the compliance control method can reduce the amount of energy for the foil propulsion and is beneficial for the energy saving design for future BAUVs. *Copyright © 2008 IFAC*

Keywords: biomimetic, underwater vehicles, compliance control, propulsive efficiency, oscillating foil

1. INTRODUCTION

Autonomous underwater vehicles (AUVs) have been used in many undersea missions, such as underwater survey and surveillances. Conventional AUVs' have drawbacks of low propulsive efficiency and poor maneuverability.Biomimetic autonomous underwater vehicles (BAUVs) are designed on the basis of mimicking the motion of fish given their ability to precisely hover and turn swiftly (Guo, 2006).

In this work, a scheme is developed to reduce propulsive cost of a foil oscillating in sway and yaw motion. By evaluating the required input energy of an actuator through the use of simulations, it is verified that this method is feasible to save energy for the propulsion of BAUVs. An overview of the swimming mechanisms of fish is presented in the review of fish swimming modes for aquatic locomotion (Sfakiotakis, *et al.*, 1999; Colgate and Lynch, 2004). Fish swim using: (a) body and/or caudal fin (BCF) locomotion, or (b) median and/or paired fin (MPF) locomotion. MPF locomotion is generally employed at low speed, offering better maneuverability and propulsive efficiency, while BCF movement is used to achieve higher thrust and accelerations. Both BCF and MPF locomotion are based on a continuous set of swimming modes: undulation and oscillation. Oscillation can be derived from increasing the wavelength of undulation. Taylor *et al.* (2003) presented that flying and swimming animals both operate within the interval 0.2~0.4 of the Strouhal number, *St*, when cruising because natural selection is likely to tune animals for high propulsive efficiency. By observing the wake structures, his team made the prediction for root-flapping and heaving hinged flat plates at varying *St*, and tested it by analyzing *St* of 42 species from bird, bat and insect families. Also, they confirmed their results using the Monte Carlo method. Streitlien. and Triantafyllou (1995) presented the closed-form expressions for force and moment on a Joukowski foil in arbitrary motion in a two dimensional potential flow. The wake from the foil is modelled as a trail of discrete point vortices which are

continually released and free to convect. By using conformal mapping and complex potential theory, the velocities of the vortices could be obtained. Anderson *et al.* (1998) studied the thrust produced through force and power measurements to classify the principal characteristics of flow around a harmonically oscillating foil. Their experimental results agreed to linear and nonlinear inviscid solutions over a certain range. Visualization data was obtained through digital particle image velocimetry. Hogan (1984) demonstrated the adaptive control of mechanical impedance in humans and examined the postulate that the central nervous system controls mechanical impedance. He modelled and analyzed the simultaneous activation of antagonist muscles in the maintenance of upright position of the forearm and hand. Theoretical prediction of antagonist co-activation and experimental observations were presented. Supported by additional kinematical analysis, Rome *et al.* (1993) concluded that most of the steady swimming power came from the posterior musculature and relatively little came from the anterior musculature, which was contradictory to the previous hypotheses. The main reason of low power generated in anterior region was that the small strain reduced output work and muscles did not relax sufficiently fast in this situation. Also, Rome (2005) extracted the principles of actuation from several studies of the fish muscular system and characterized the differences between artificial and real muscles, which can provide some suggestions for designing and constructing AUVs. Blickhan and Cheng (1994) re-evaluated the question of energy storage of cetaceans by using a model with more realistic calculation of hydrodynamic force. His team calculated the optimum compliance and compared it to the actual compliances observed in the cetaceans. The result showed that the energy cost can be reduced by the elastic mechanism in the cetaceans. Harper *et al.* (1998) modelled an oscillating foil connected to translational and rotational actuators with springs. His team derived not only the expressions of the optimal spring constants but also a set of necessary and sufficient conditions for stability, given that the use of the spring may lead to unstable foil. Under the condition of optimal spring constant, the use of springs can reduce energy costs. Moreover, Murray *et al.* (2003) modelled a foil that was supported by a translational spring and driven by a single rotational actuator. His team discussed the effects of variations in spring stiffness and the minimum oscillation frequency required producing positive thrust.

This paper proposes a novel way of turning the spring stiffness in real time by feeding back hydrodynamic forces and moment acting on the tail fin. In Section 2, the mechanics of an oscillating foil is described. Section 3 presents the formulation of energy storage by elastic elements. The method for reducing energy using a spring with variable compliance is provided. Simulation results for the verification of the methods are then presented in Section 4. Also, in Section 4, some observations regarding the energy requirement for turning a variable compliance spring are discussed. Finally, Section 5 provides concluding remarks.

2. HYDRODYNAMICS OF AN OSCILLATING FOIL

Consider a foil with chord length c, moving forward with constant speed U_f and performing harmonic sway and yaw motion in a two dimensional flow. To define the parameters of the foil, as shown in Fig. 1, let $O-XY$ and $o-xy$ be the space-fixed and body-fixed coordinate system. The sway motion is:

$$h = h_0 \cos(\omega t) \tag{1}$$

And, the yaw motion is:

$$\theta = \theta_0 \cos(\omega t + \varphi) \tag{2}$$

Where, h_0 and θ_0 are the amplitude of sway and yaw motion, ω is the frequency, and φ is the phase angle between sway and yaw motion. The foil yaws about a point O_b whose distance from the leading edge is b. The foil is subject to the hydrodynamic forces $X(t)$ and $Y(t)$ in $X-$ and $Y-$ directions respectively, and a moment $M(t)$ (positive for counter-clockwise). With an oscillating period T, the time-averaged force F_{thrust} is:

$$F_{thrust} = \frac{1}{T}\int_0^T X(t)\,dt \tag{3}$$

And, the average input power per cycle is:

$$P = \frac{-1}{T}\left(\int_0^T Y\frac{dh}{dt}dt + \int_0^T M\frac{d\theta}{dt}dt\right) \tag{4}$$

Several non-dimensional terms and parameters are defined as follows (Anderson, *et al.*, 1998).

C_T, the thrust coefficient, is defined as,

$$C_T = \frac{F_{Thrust}}{\frac{1}{2}\rho U_f^2 c} \tag{5}$$

where ρ denotes the fluid density, C_P, the power coefficient, is defined as,

$$C_P = \frac{P}{\frac{1}{2}\rho U_f^3 c} \tag{6}$$

η , the propulsive efficiency, is defined as,

$$\eta = C_T \Big/ C_{Power} = \frac{F_{Thrust} U_f}{P} \tag{7}$$

b^* is the distance of the point O_b from leading edge divided by the chord length, $b^* = b/c$. h^* is the sway amplitude-to-chord ratio $h^* = h_0/c$, and St is Strouhal number is defined by,

$$St = \frac{fA}{U_f} \tag{8}$$

In Eq. (8), $f = \omega/(2\pi)$ denotes the frequency of the foil in Hz, and $A = 2h_0$, denotes the characteristic width of the created jet flow. Let St_{TE} be the Strouhal number based on the total excursion of the trailing edge of the foil, A_{TE} , that is,

$$St_{TE} = \frac{fA_{TE}}{U_f} \tag{9}$$

A foil is assumed to be swimming through a two-dimensional, inviscid, incompressible, and irrotational fluid. Also, the fluid is at rest at infinity. Under these assumptions, the flow field, hydrodynamic forces, and moment that act on the foil are determined using potential flow theory. Solutions were presented in Streitlien. and Triantafyllou (1995). The forces on the foil along the x - and y -axis can be calculated by

$$F_x + iF_y = i\int_\Sigma p dz \tag{10}$$

And the counter-clockwise moment about the foil centre point is

$$M_0 = \mathrm{Re}\left\{\int_\Sigma pz\overline{dz}\right\} \tag{11}$$

where the pressure distribution on the foil p needs to be calculated and its distribution is given by (Milne-Thomson 1968).

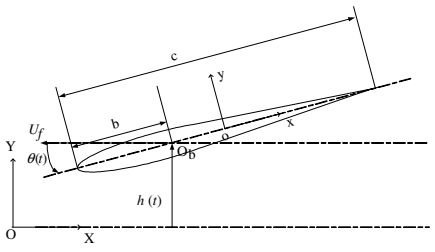

Figure 1: Definition of principal parameters for the oscillating foil.

3. ENERGY STORAGE BY ELASTIC ELEMENTS

Figure 3 depicts a foil driven by lateral and rotational actuators via springs. The springs are attached to the point O_b where h and θ measure the lateral and rotational motion of the point. The inertial forces and moment of the foil are calculated as:

$$m\left(\dot{U}_b - \Omega_b V_b\right) - mx_G{\Omega_b}^2 = f_{ix} \tag{12}$$

$$m\left(\dot{V}_b + \Omega_b U_b\right) + mx_G\dot{\Omega}_b = f_{iy} \tag{13}$$

$$I_{zz}\dot{\Omega}_b + mx_G\left(\dot{V}_b + \Omega_b U_b\right) = M_i \tag{14}$$

where

$$U_b = U_f\cos\theta + \dot{h}\sin\theta \tag{15}$$

$$V_b = -U_f\sin\theta + \dot{h}\cos\theta \tag{16}$$

$$\Omega_b = \dot{\theta} \tag{17}$$

In Eqs. (12)- (14), f_{ix} represents the inertial force on O_b in the x direction, f_{iy} represents the inertial force on O_b in the y direction, and M_i denotes the inertial moment on O_b . m is the mass of the foil, I_{zz} is the inertia moment acting on O_b , and x_G is the position of the centre of mass. The positions h_a and θ_a are controlled by actuators. The force and torque applied by the actuators are

$$F_a = (h_a - h)/C_l \tag{18}$$

$$M_a = (\theta_a - \theta)/C_r \tag{19}$$

where C_l is the lateral spring compliance, and C_r is the compliance of the rotational spring. From Eqs. (12)- (19), the equations of motion are

$$f_{ix}\sin(\theta) + f_{iy}\cos(\theta) = F_i = Y + F_a \tag{20}$$

$$M_i = M + M_a \tag{21}$$

where

$$Y = F_x\sin(\theta) + F_y\cos(\theta) \tag{22}$$

$$M = M_0 + F_y(c/2 - b) \tag{23}$$

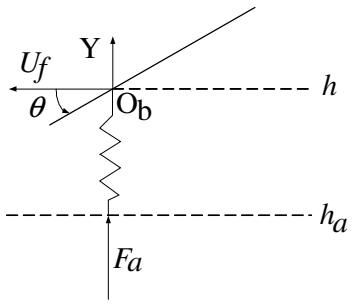

Figure 2: Lateral and rotational motions of the foil.

Swaying and yawing motions of the foil are both sinusoidal. Inertial forces and moment derived with respect to the pivot point O_b for the foil have a sinusoidal form as presented in Eqs. (24), (25). Hydrodynamic forces and moment with respect to O_b are made up of motion with frequency ω, and frequency components higher than ω, as indicated in Eqs. (26) and (27).

$$F_i = F_{i0}\cos(\omega t + \varphi_1) \tag{24}$$

$$M_i = M_{i0}\cos(\omega t + \varphi_2) \tag{25}$$

$$Y = Y_1\cos(\omega t + \varphi_{Y1}) + \sum_{k_l=2}^{n_l} Y_{k_l}\cos(\omega_{Yk_l} t + \varphi_{Yk_l}) \tag{26}$$

$$M = M_1\cos(\omega t + \varphi_{M1}) + \sum_{k_m=2}^{n_m} M_{k_m}\cos(\omega_{Mk_m} t + \varphi_{Mk_m}) \tag{27}$$

where F_{i0} and M_{i0} are amplitudes of the inertial forces and moment, respectively. φ_1, φ_2 are phase leads of inertial forces and moment with respect to the sway motion, respectively. Y_{k_l}, $k_l = 1,..,n_l$ is the amplitude of lateral hydrodynamic force which has the frequency component, $\omega_{Y_{k_l}}$. M_{k_m}, $k_m = 1,..,n_m$ is the amplitude of hydrodynamic moment which has the frequency component, ω_{Mk_m}. ω_{Yk_l}, ω_{Mk_m} are frequency components of force and moment exerted on the foil due to hydrodynamics, and φ_{Yk_l}, φ_{Mk_m} are phase angles, respectively. The total input power from actuators is given as:

$$P_{al} + P_{ar} = F_a\dot{h}_a + M_a\dot{\theta}_a \tag{28}$$

where $P_{al} = F_a\dot{h}_a$, represents the power input from the lateral actuator, and $P_{ar} = M_a\dot{\theta}_a$ is the power input from the rotational actuator. For small-amplitude foil oscillations, hydrodynamic forces and moment can be approximated by signals with the oscillating frequency component, ω (Blickhan and Cheng, 1994), that is, Y_{k_l} and M_{k_m} are identically zeros. With a constant compliance C_l of the lateral spring, the lateral power input can be calculated by

$$\begin{aligned} P_{al} &= F_a\dot{h}_a \\ &= (F_i - Y)\left\{\frac{d}{dt}\left[(F_i - Y)C_l + h\right]\right\} \\ &= (F_i - Y)\left[\dot{h} + (\dot{F}_i - \dot{Y})C_l\right] \\ &= P_0 + P_1\cos 2\omega t + P_2\sin 2\omega t \\ &= P_0 + P_3\cos(2\omega t + \varphi_{al}) \end{aligned} \tag{29}$$

where φ_{al} is the phase lead of the lateral power input with respect to the sway motion, and

$$P_0 = \frac{h_0\omega}{2}(F_{i0}\sin\varphi_1 - Y_1\sin\varphi_{Y1}) \tag{30}$$

$$\begin{aligned} P_1 &= \frac{1}{2}(Y_1h_0\omega\sin\varphi_{Y1} - F_{i0}h_0\omega\sin\varphi_1) \\ &\quad + C_l[\frac{-F_{i0}^2}{2}\omega\sin 2\varphi_1 \\ &\quad + Y_1F_{i0}\omega\sin(\varphi_1 + \varphi_{Y1}) - \frac{Y_1^2}{2}\omega\sin 2\varphi_{Y1}] \\ &= x_{11} + C_l x_{12} \end{aligned} \tag{31}$$

$$\begin{aligned} P_2 &= \frac{1}{2}(Y_1h_0\omega\cos\varphi_{Y1} - F_{i0}h_0\omega\cos\varphi_1) \\ &\quad + C_l[\frac{-F_{i0}^2}{2}\omega\cos 2\varphi_1 \\ &\quad + Y_1F_{i0}\omega\cos(\varphi_1 + \varphi_{Y1}) - \frac{Y_1^2}{2}\omega\cos 2\varphi_{Y1}] \\ &= y_{11} + C_l y_{12} \end{aligned} \tag{32}$$

$$P_3 = \frac{P_1}{\cos\varphi_{al}} \tag{33}$$

$$\varphi_{al} = \tan^{-1}\left(\frac{-P_2}{P_1}\right) \tag{34}$$

The goal of implementing the spring mechanism is to use the actuation power more efficiently for producing propulsion. Negative power during the cycle generates braking to the motion. Eliminating negative power actuation results in less power requirements from the actuator. When $P_0 = P_3$, the power function is positive in all cycles. To find the minimum of P_3, let

$$\frac{\partial P_3}{\partial C_l} = 0 \tag{35}$$

which gives the value of optimal compliance constant for the lateral spring, C_{lop}.

$$C_{lop} = \frac{-(x_{11}x_{12} + y_{11}y_{12})}{x_{12}^2 + y_{12}^2} \tag{36}$$

The same procedure can be followed to derive the optimal compliance constant for the rotational spring, For foils oscillating with large amplitudes, hydrodynamic forces and moment have higher frequency components other than the oscillating frequency. In order to reduce the influence of high frequency components, the use of springs with variable compliance is proposed. The compliance of springs with a variable component in addition to the constant component is defined as:

$$C_l = C_{lop} + C_{l\Delta} \tag{37}$$

where $C_{l\Delta}$ is the increments of the compliance due to the effect of high frequency hydrodynamic forces. The positive work condition for the lateral power gives

$$\begin{aligned} P_{al} &= F_a \dot{h}_a \\ &= (F_a)\left[\dot{h} + \dot{F}_a C_z + F_a \dot{C}_{l\Delta}\right] \geq 0 \end{aligned} \tag{38}$$

By adding and subtracting the positive power $P_0 + P_3 \cos(2\omega t + \varphi_{al})$, which contain two times of the oscillating frequency component, ω, a sufficient condition for positive power input is then established by letting (F_a) $[\dot{h} + \dot{F}_a C_l$ $+F_a \dot{C}_{l\Delta}]$ $-[P_0 +$ $P_3 \cos$ $(2\omega t + \varphi_{al})]$ $= 0$ The rule for tuning the compliance can then be obtained as follows.

$$\begin{aligned} \dot{C}_{l\Delta} = &-\frac{\dot{F}_a}{F_a} C_{l\Delta} - \frac{\dot{F}_a}{F_a} C_{lop} \\ &-\frac{1}{F_a}\dot{h} + \frac{1}{F_a^2}[P_0 + P_3 \cos(2\omega t + \varphi_{al})] \end{aligned} \tag{39}$$

Compared with the input power using constant compliance defined in Eq. (29), it is important to note that as the spring has a variable compliance, an additional amount of energy, P_{sl} for turning the spring compliance is required.

$$P_{sl} = C_{l\Delta} F_a \dot{F}_a + \dot{C}_{l\Delta} F_a^2 \tag{40}$$

P_{sl} is the power associated with the variable compliance component, $C_{l\Delta}$ and $\dot{C}_{l\Delta}$. Furthermore, based on the physical condition, the magnitude of the compliance is bounded. Maximum and minimum compliances are determined by the spring's specifications. Here, they are chosen to be 0 and ∞, respectively. Furthermore, to find the variable component of the rotational spring, $C_{r\Delta}$ and the power associated with the variable component in the rotational spring, P_{sr} the same derivation procedure for the lateral degree of freedom applies.

4. SIMULATIONS

To show the effectiveness of the control method, several harmonic motions of the oscillating foil are performed and their input power requirements are evaluated. Motion parameters of an oscillating foil for the simulation tests are chosen based on the experimental setup and results from Anderson *et al.*, 1998. In their work, some parameters were suggested for producing propulsive force with high energy efficiency. Those tests were performed on a NACA 0012 foil with a chord length of 10 cm. The density of the foil is set to 1000 kg/ m^3, the density of water. The mass of the foil, m is 0.8221kg, and the moment of inertia I_{zz} is 0.000537 $kg \cdot m^2$. The position of the centre of mass, x_G is 0 m. The one-third-chord point is adopted as the pivot point and the phase angle φ between sway and yaw motion is set to be 90°. Figure 3 illustrates the propulsion efficiency of an oscillating foil under the condition: $h^* = 0.75$, $\alpha_0 = 15^\circ$, $\varphi = 90^\circ$. At $\varphi = 90^\circ$, the nominal angle of attack α_0, can be approximated to be

$$\alpha_0 = \arctan\left(-\frac{\omega h_0}{U_f}\right) - \theta_0 \tag{41}$$

Thrust coefficient, power coefficient and propulsive efficiency were calculated using Eqs. (3)- (7). From the data, foil oscillations that are in the range of $0.25 < St_{TE} < 0.4$ result in better performance both in thrust production and energy efficiency. Larger thrust can be produced at higher St_{TE}, but the efficiency decays at higher St_{TE}. Figure 4 shows the savable energy of (a) lateral and (b) rotational actuator per cycle under various St_{TE}. The solid lines represent the proportions of energy that can be saved from the actuators (i.e. twice of the amount of the negative work divided by the sum of the positive and negative work for both lateral and rotational motions with no coupling to springs). The marks o and $\triangleleft$ represent the proportions of savable energy from actuators coupled with springs with constant and variable compliances, respectively. In the range of $0.1 < St_{TE} < 0.27$, lateral spring compliances with constant values can be obtained and almost all lateral negative work can be recovered. In the range of $0.33 < St_{TE} < 0.46$, due to the effect of high frequency components in the hydrodynamic forces and moment, the lateral compliance with a constant value cannot be obtained. Instead, by using springs with variable compliances results in good reduction in negative work. These simulation data reveal that an actuator coupled with a spring with variable compliance can reduce energy cost when thrust production has a higher priority than swimming efficiency. However, at very large St_{TE}, high frequency components in the hydrodynamic forces and moment have large amplitudes compared to the amplitude of the oscillating frequency component. In this case, the proposed technique calculates some negative compliances which are no longer feasible for practical applications.

5. CONCLUSION

This study describes a compliance control scheme for the caudal joint motion of a BAUV. A foil is

modelled as a tail oscillating in sway and yaw motions. The foil is connected to lateral and rotational actuators with springs. By controlling compliances of the lateral and rotational springs, the required input energy of the actuators can be reduced. A sufficient condition is derived under which the averaged work done by actuators remain positive. Compliance control scheme is then derived based upon the constraint condition provided by the sufficient condition. Hydrodynamic forces and moment that act on the foil are determined by calculations using potential flow theory. Numerical simulations reveals that by controlling compliance of attached springs, required work for actuating the foil can be reduced by an amount of 5-10%. A BAUV illustrated in Figure 5 having variable compliance actuators are being built for testing the concept presented in this article.

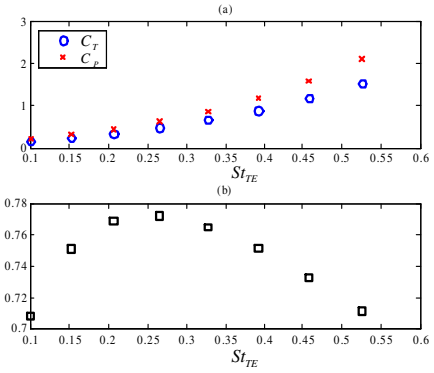

Figure 3: (a) Thrust and power coefficients (b) efficiency under various St_{TE} with $h^* = 0.75$, $\alpha_0 = 15^\circ$ and $\varphi = 90^\circ$.

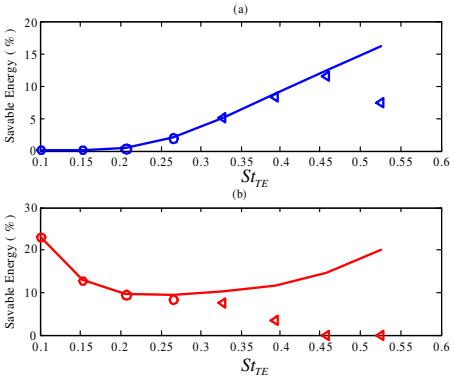

Figure 4: Lateral (a) and rotational (b) savable energy per cycle under various St_{TE} with $h^* = 0.75$, $\alpha_0 = 15^\circ$ and $\varphi = 90^\circ$. Solid lines represent savable energy and o and $\triangleleft$ represent energy saved using actuators coupled with springs of constant and variable compliances, respectively.

ACKNOWLEDGMENT

The authors would like to thank the National Science Council of the Republic of China, Taiwan, for financially supporting this research under Contract No. NSC90-2611-E002-030.

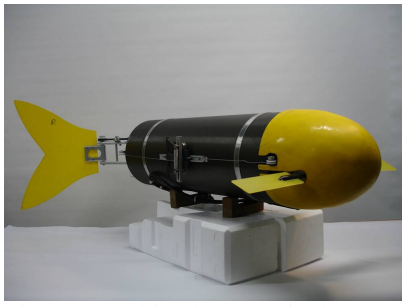

Figure 5: BAUV which has a variable-compliance caudal joint

REFERENCES

Anderson, J. M., K. Streitlien, D. S. Barrett and M. S. Triantafyllou, (1998). Oscillating foils of high propulsive efficiency. *Journal of Fluid Mechanics,* **Vol. 360**, pp. 41-72.

Blickhan R. and J. Y. Cheng, (1994). Energy storage by elastic mechanisms in the tail of large swimmers-a re-evaluation. *Journal of Theoretical Biology*, **Vol. 168**, pp. 315-321.

Colgate, J. E., K. M. Lynch, (2004). Mechanics and control of swimming: a review. *IEEE J. Oceanic Eng.*, 2004, **Vol. 29, No. 3**, pp. 660-673.

Guo J., (2006). A waypoint-tracking controller for a biomimetic autonomous underwater vehicle. *Ocean Engineering*, **33**, pp. 2369-2380.

Harper, K. A., M. D. Berkemeier and S. Grace, (1998). Modeling the dynamics of spring-driven oscillating-foil propulsion. *IEEE Journal of Ocean Engineering*, **Vol. 23, No. 3**, pp.285-296.

Hogan, N., (1984). Adaptive control of mechanical impedance by coactivation of antagonist muscles. *IEEE Transactions on Automatic Control*, **Vol. AC-29**, **No. 8**, pp. 681-690.

Milne-Thomson, L. M., (1968). *Theoretical Hydrodynamics*, Macmillan, New York.

Murray, M. M. and L. E. Howle, (2003). Spring stiffness influence on an oscillating propulsor. *Journal of Fluids and Structures*, **Vol. 17**, pp. 915-926.

Rome, L. C., D. Swank and D. Corda, (1993). How fish power swimming. *Science*, **Vol. 261**, pp. 340-343.

Rome, L. C., (2005). Principles of actuation in the muscular system of fish. *IEEE Journal of Oceanic Engineering*, **Vol. 30, No. 3**, pp. 630-646.

Sfakiotakis, M., D. M. Lane and J. B. C. Davies, (1999). Review of fish swimming modes for aquatic locomotion, *IEEE Journal of Oceanic Engineering*, **Vol. 24, No. 2**, pp. 237-252.

Streitlien, K. and M. S. Triantafyllou, (1995). Force and moment on a Joukowski profile in the presence of point vortices. *AIAA Journal*, **Vol. 33, No. 4**, pp. 603-610.

Taylor, G. K., R. L. Nudds and A. L. R. Thomas, (2003). Flying and swimming animals cruise at a Strouhal number tuned for high power efficiency. *Nature*, **Vol. 425**, pp. 707-711.